

Characteristics of an optically activated pulsed power GaAs(Si:Cu) switch obtained by two-dimensional modeling

Phillip J. Stout^{a)} and Mark J. Kushner^{b)}

University of Illinois, Department of Electrical and Computer Engineering, 1406 West Green Street, Urbana, Illinois 61801

(Received 24 June 1994; accepted for publication 5 December 1994)

Photoconductive semiconductor switches (PCSS) have high-voltage hold-off (many to tens of kilovolts) and fast current rise times (< 1 ns). However, lock-on, nonuniformities in the electric field, and filamentary current flow across the device when switching at high fields (~ 10 kV/cm) have been reported. These observations raise concerns about the scaling of PCSS to high currents (tens of kiloamperes). To investigate these issues a two-dimensional time dependent computer model of a GaAs PCSS with Si and Cu doping has been developed. The model solves the continuity equations, the bulk energy equation, Poisson's equation for the electric field, and a circuit equation for external currents. Physical effects in the model include band-to-band impact ionization, trap impact ionization, photoionization, and negative differential resistance. Computed characteristics of GaAs(Si:Cu) switches will be reported. Experimentally observed electric-field distributions are explained. © 1995 American Institute of Physics.

I. INTRODUCTION

Pulsed power switches (tens of kilovolts, hundreds of amperes to tens of kiloamperes) have traditionally been gas discharges such as thyatrons and spark gaps.¹ Photoconductive semiconductor switches (PCSS) are being investigated as alternatives to gas phase switches. PCSS have high-voltage hold-off (many to tens of kilovolts) and circuit limited rise times of less than a nanosecond. The switches are essentially jitter-free. Their jitter is typically limited only by the jitter of the trigger source, a pulsed laser. Photoconductive switches have been used to obtain picosecond switching in a low power setting.² The goal of current investigations is to utilize the rapid photoconductivity of semiconductors at higher powers. PCSS have found many potential applications including the generation of ultrawide band pulses for radar applications.^{3,4}

Experimental observations of GaAs PCSS have shown the presence of nonuniformities in the electric field,⁵⁻⁷ filamentation of current flow across the device when switching at high fields (~ 10 kV/cm),^{8,9} and a "lock-on" effect.¹⁰⁻¹² Filamentation has caused concern about the scaling of PCSS to large currents. Filamentation can result in higher carrier densities by constricting currents to smaller cross-sectional areas. Local heating by filaments and point attachment to contacts can result in damage to the device. Lock-on, which occurs when the switch is operated above a characteristic electric field, results in current continuing to flow after the termination of the activating optical pulse. In the absence of lock-on bulk GaAs PCSS would open in nanoseconds or less. Also, at these high fields the amount of light required to close the switch is reduced from the amount needed at low fields. Lock-on, though associated with optical trigger gain, is generally not desirable since the ability to control the current using the incident laser flux is compromised.

PCSS operate by modulating the conductivity of a semiconductor by photoabsorption through the creation of electron-hole pairs. Shining band-gap radiation from a laser on the sample generates an electron-hole plasma which conducts the switch current and closes the switch. When the laser pulse is terminated, and in the absence of lock-on, the conductivity rapidly decreases due to electron-hole recombination. If a fast opening switch is desired, a short electron-hole pair (EHP) lifetime is required. Direct-gap semiconductors are therefore candidates for fast opening switches. These semiconductors have radiative lifetimes of a few nanoseconds and in specially prepared semi-insulating GaAs the EHP lifetime can be < 1 ns.³ To maintain conductivity for times longer than the EHP lifetimes, the device must be continuously illuminated or a process such as carrier multiplication (e.g., avalanche) or possibly double injection¹³ must occur. One would therefore like a means to extend the closed phase of the switching cycle for a semiconductor having a short EHP lifetime without increasing the laser power. The GaAs(Si:Cu) bulk optical semiconductor switch (BOSS) developed by Schoenbach addresses this issue.¹⁴

In the BOSS, a deep acceptor (Cu) is compensated by a shallow donor (Si). To close the switch the photon energy of the switching laser is selected to be large enough to cause emission of electrons from the acceptor level and the valence band via the acceptor level. This "on" light increases the number of free electrons and holes, thereby increasing the conductivity and closing the switch. When the on illumination of the sample is terminated, the switch can remain conductive by selecting an acceptor that is an inefficient electron trap and an efficient hole trap. The BOSS can remain closed for hundreds of nanoseconds to a few microseconds. The switch is opened by photoquenching the free electrons by selective photoexcitation of holes from the deep acceptor level. This is possible by selecting an "off" photon energy that is large enough to stimulate hole emission from the acceptor but small enough to prevent electron emission. The

^{a)}Present address: CFD Research Corporation, 3325 Triana Blvd., Huntsville, AL 35805.

^{b)}Author to whom correspondence should be addressed; Electronic mail: mjk@uiuc.edu

holes so created quickly recombine with free electrons which were previously maintaining the conductivity, thereby opening the switch.

To investigate scaling issues of the BOSS a two-dimensional time dependent computer model has been developed. The model solves the continuity equations for electrons and holes, Poisson's equation for the electric potential, a global energy equation, and circuit equations. Using results from the model, processes leading to experimentally observed nonuniformities in electric field and current flow are discussed.

II. DESCRIPTION OF THE MODEL

The model is a two-dimensional time dependent simulation of electron and hole currents, and densities of traps. The general flow of the model is as follows. The continuity equations for electrons, holes, and impurities and the energy equation for the lattice are solved on a rectilinear mesh having variable spacing using finite differencing. Flux conservative donor cell techniques are used to represent the drift and diffusion terms. The electron and hole fluxes crossing into the contacts are integrated to obtain the current through the device. A circuit equation is included to provide the voltage across the device. In practice, the current is generally inductively limited flowing into a $50\ \Omega$ load. Poisson's equation is solved for the electric potential using an implicit successive-overrelaxation technique.¹⁵

The acceptors used in the model are Cu_A (0.14 eV relative to the valence-band edge) and Cu_B (0.44 eV). The donors are Si (0.0058 eV relative to the conduction-band edge), $EL2$ (0.83 eV), and $EL5$ (0.41 eV). In practice, the rate equations do not include Si. Since Si is a shallow donor, it is assumed to be completely ionized at all times at room temperature. Photoionization resulting from the on and off laser pulses (1.1 and 0.7 eV photon energy, respectively) is included in the model. The energies of the traps relative to the GaAs band edges determine which traps are photoionized. The on laser induces electron and hole emission from all traps. The off laser flux induces hole emission from Cu_A and Cu_B , electron and hole emission from $EL2$ and RC , and electron emission from $EL5$. Trapping and photoionization cross sections are noted in Ref. 16. The recombination rate coefficient used in the model, however, is $7 \times 10^{-6}\ \text{cm}^3/\text{s}$ which is four orders of magnitude greater than used by Ko.¹⁶ Stoudt¹⁷ has shown that engineering the recombination center density plays an important role in rapid opening times (subnanosecond). By using neutron irradiated material which introduces recombination centers, Stoudt was able to reduce opening times in GaAs from tens of nanoseconds to subnanosecond. The intent of this work is to investigate subnanosecond switching time scales as demonstrated by Stoudt. The recombination rate coefficient we have used is therefore an effective recombination rate, which reflects the recombination rates due to processes such as introduced recombination centers as well as the intrinsic recombination rate cited in Ref. 16.

An energy conservation equation including thermal conduction and joule heating was used to obtain the lattice temperature. Given the fast energy relaxation times of electrons

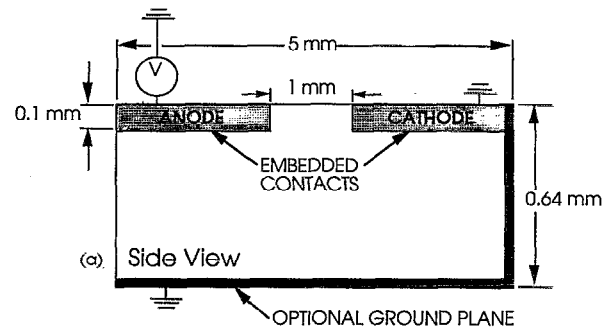


FIG. 1. Lateral switch geometry used in the model. The device has a depth of 4 mm. The right and bottom borders of the device may be grounded in a stripline configuration.

and holes ($\tau_e \approx \tau_h \approx 10^{-12}\ \text{s}$) compared to the simulation times of interest (tens of nanoseconds), the electron and hole temperatures will differ little from that of the lattice. The thermal conductivity is assumed to be spatially uniform at $0.46\ \text{J/cm s K}$. The specific heat is $0.35\ \text{J/g K}$. The temperature of all boundaries was set to 300 K.

As with other materials with satellite valleys in their conduction bands, GaAs exhibits negative differential conductivity, making the carrier velocities a nonlinear function of the electric field. This negative differential conductivity can lead to electric-field instabilities due to the Gunn effect. In GaAs, the steady-state drift velocity reaches a maximum at a field of $\approx 3\ \text{kV/cm}$ and then decreases, eventually saturating at high fields. Due to saturation of the drift velocity, substantially lower mobilities are obtained at high electric fields. The electron drift velocity v_e in the model is a fit of experimental data¹⁸ having a saturation velocity of $v_s = 7 \times 10^6\ \text{cm s}^{-1}$. The hole velocity is a linear function of the electric field until the saturation velocity is reached ($v_p = 8.0 \times 10^6\ \text{cm s}^{-1}$ for $E \geq 2.0 \times 10^4\ \text{V cm}^{-1}$). The intrinsic carrier density n_i and the thermal velocity v_{th} are functions of the lattice temperature. The band-to-band impact ionization coefficient α_i is approximated as being a function of the local electric field. n_i and α_i in the model are functional fits of data from Sze.¹⁸ For our conditions, avalanche will produce $1/n_e \cdot dn_e/dt = 10^7\ \text{s}^{-1}$ when $E = 1.38 \times 10^5\ \text{V cm}^{-1}$. Trap impact ionization in the model produces only electrons. The trap impact ionization cross section σ_t has an exponential dependence on the electric field with the characteristic field E_t , $\sigma_t = \sigma_{t0} \exp[-E_t/|E|]\ \text{cm}^2$. The value of E_t was approximated by the relative position of the trap energy level. The maximum cross section σ_{t0} was chosen for effect.

III. COMPUTED SWITCHING CHARACTERISTICS

The lateral switch geometry used in the model is patterned after the work of Schoenbach *et al.*⁷ and is shown in Fig. 1. The right side and bottom of the switch are treated as being either floating (isolated) or grounded. The embedded anode and cathode are both current injecting. The electric fields normal to floating surface are set to zero. In our simulations the PCSS is doped $10^{10}\ \text{cm}^{-3}$ n type with $N_{Si} \approx N_{Cu} = 10^{16}\ \text{cm}^{-3}$. The on laser pulse has a Gaussian

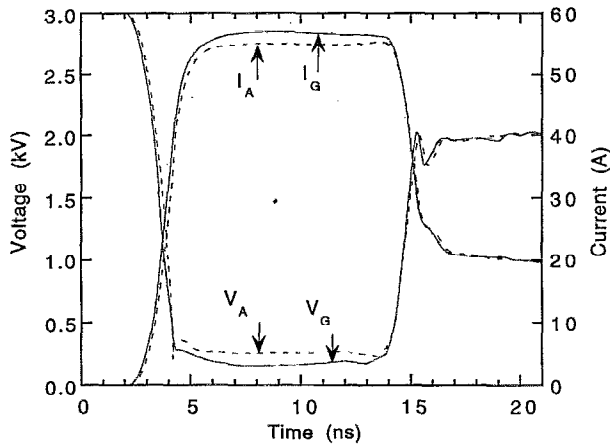


FIG. 2. Current-voltage characteristics for the abrupt (I_A , V_A) and graded (I_G , V_G) contact cases. The on laser pulse peaks at 6 ns. The off laser pulse peaks at 16 ns. The graded contact case closes to a lower voltage given less severe velocity overshoot for electrons near the anode.

temporal shape centered at 6 ns (FWHM=2 ns) with a maximum intensity of $\approx 3 \text{ MW cm}^{-2}$. The off laser is centered at 16 ns and has a maximum intensity of $\approx 4 \text{ MW cm}^{-2}$. The laser pulses are spatially Gaussian with a FWHM of 1 mm centered between the anode and cathode.

Current and voltage during a switching cycle using the grounded lateral geometry with abrupt contacts are shown in Fig. 2. Upon application of the on laser pulse, photodetachment of the ionized Cu acceptors introduces electrons into the conduction band. The applied voltage across the switch decreases from 3 kV to $\approx 250 \text{ V}$. The current is switched from milliamperes to a circuit limited value of $\approx 55 \text{ A}$. Upon application of the off laser pulse, the Cu acceptors are reionized. This action produces holes in the valence band, which provides recombination partners for the conduction electrons. Note that in the example in Fig. 2 the fluence of the off laser was purposely chosen to produce fewer than the required number of holes to completely deplete electrons in the conduction band by recombination. The end result is that the switch opens to only 2 kV. The switch will open to the line voltage slowly as the Cu acceptors are thermally ionized, generating holes in the valence band. The current density is maximum at $\approx 5 \text{ kA/cm}^2$ though it is spatially nonuniform. In general, experimental devices have spatially averaged current densities of $\approx 2 \text{ kA/cm}^2$.^{3,7}

Electric fields in BOSS devices have been measured by Schoenbach *et al.* using a photoabsorption technique based on the Franz-Keldysh effect.⁷ Transient nonuniformities in the electric field were observed for voltage pulses above a threshold (above $\approx 3 \text{ kV}$ in the lateral geometry) with more severe nonuniformity as the voltage was increased. Electric-field enhancement before laser activation is observed near the cathode. As the hold-off voltage is increased, enhancement is also seen near the anode. At laser activation increased photoabsorption is observed near the anode (indicating an increased electric field there).

A time evolution of the electric field for the grounded abrupt contact case is shown in Fig. 3 for the same condi-

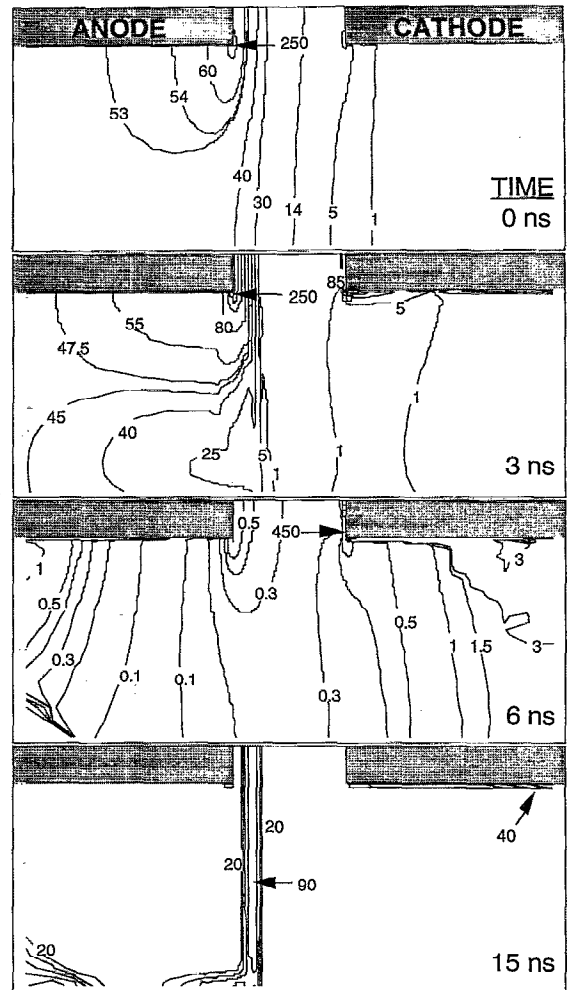


FIG. 3. Time evolution of electric field (kV cm^{-1}) for the grounded abrupt contact case for the conditions of Fig. 2. At $t=0$, electric-field enhancement at the anode is geometrical. During the on laser pulse, the electric-field enhancement switches to the cathode as a depletion region is formed there. During the off laser pulse, the region of electric-field enhancement migrates to the anode as residual carriers are swept out of the bulk.

tions as in Fig. 2. The electric field is initially enhanced at the sharp edge of the embedded anode. There is less enhancement at the grounded cathode due to proximity of the grounded base. As the on laser is applied ($t=3 \text{ ns}$) the introduction of mobile carriers between the contacts increases the conductivity in the region, thereby reducing the voltage drop. The result is a compression of the electric field to the contacts adding to the geometrical enhancement at the anode. The intrinsic avalanche which occurs at the contacts due to the enhanced electric field actually acts to limit the peak electric field. This is followed by a collapse of the electric field to the cathode during the closed or on state of the switch ($t=6 \text{ ns}$) as the electrons are swept into the anode, thereby moderating the space-charge variation there. This electric-field configuration remains fairly stable during the closed phase with the electric-field enhancement as the cathode being due in large part to the high level of electron injection occurring as the switch conducts large currents.

During the off laser pulse holes are introduced between the contacts, reducing the conductivity in the region by recombination. The electric field at the cathode begins to increase due to the resulting increase in hold-off voltage. However, as the switch opens ($t=15$ ns), the region of electric-field enhancement begins to move toward the anode, progressing at the electron saturation velocity. The motion of the high electric field toward the anode results from negative differential conductivity and a traveling gradient in electron density. This gradient is produced by a reduction of electron injection at the cathode as the switch opens, and the introduction of holes between the contacts which reduce the electron density through recombination. A Gunn domain results from this electron-density variation. These trends concur well with the experimental observations.⁵⁻⁷

High electric-field regions with high carrier concentration can cause substantial joule heating. Severe local heating can damage the device, particularly at the contacts. A consequence of a moderate local increase in temperature is a decrease in the band gap. The decreasing band gap causes the intrinsic carrier concentration to increase, and increases the rate that electrons and holes are emitted from the traps. This results in larger local rates of joule heating, leading to higher temperatures. Highly nonuniform heating rates of 2×10^6 K/A s near the anode and cathode have been simulated. A short voltage pulse (20 ns duration) produces only nominal increases in local temperature. However, long current pulses (hundreds of nanoseconds to a few microseconds) coupled with high-frequency repetitive switching will result in large temperature excursions. For example, a 2 μ s current pulse with the abrupt contact device will produce local temperature increases of 200 K over ambient.

Electric-field enhancement at the contacts can result in nonuniform carrier injection and possibly provide end points for filaments to strike and degrade the contacts. One source of electric-field enhancement is simply the sharp edges of the contacts. Grading the contacts by producing a smooth transition in permittivity (by, for example, ion implantation) will reduce the field enhancement at the cathode and displace the maximum in the electric field into the bulk semiconductor. Since injection at the contacts is generally a function of electric field, providing a more uniform electric field at the contacts will promote more uniform injection at the contacts, thereby reducing the likelihood of filament formation.

To simulate graded contacts in the model, the electrical permittivity was exponentially varied from the edge of the contacts from $\epsilon/\epsilon_0=83.2$ to the bulk value (13.2) over a distance of 0.1 mm. The time evolution of the electric field for the graded contact case is shown in Fig. 4. At $t=0$ the peak of the electric field in the abrupt contact case occurs at the corner of the anode. However, the peak in the electric field is displaced into the bulk semiconductor with the graded contacts. As the switch cycle progresses the switch with the graded contacts also has a region of electric-field enhancement which collapses to the cathode ($t=3$ and 6 ns) and shifts to the anode as the switch opens ($t=15$ ns). However, the graded contact case has lower field enhancement throughout the switch cycle as compared to the abrupt contact case. The graded contact switch also closes to a lower

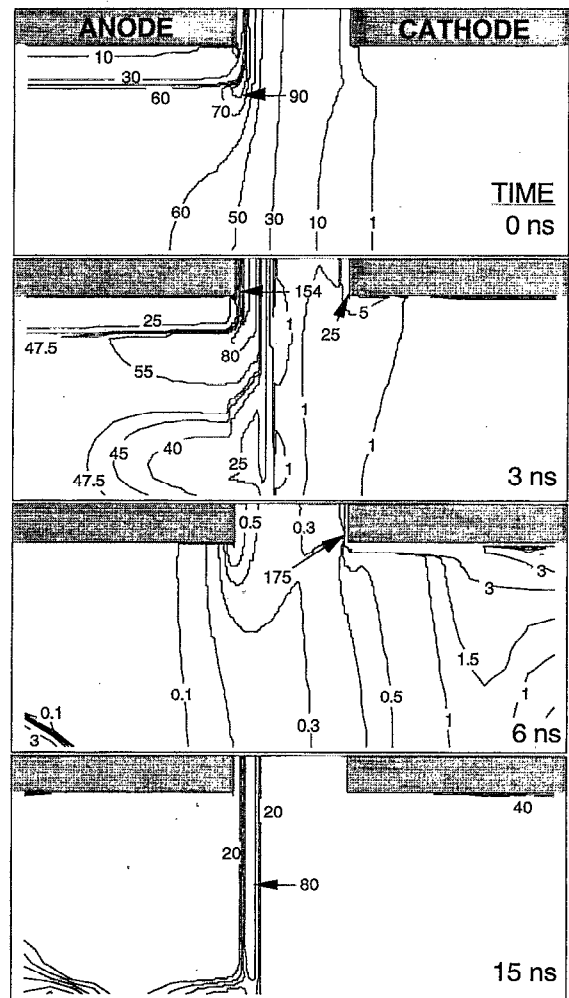


FIG. 4. Time evolution of electric field (kV cm^{-1}) for the graded contact case. At $t=0$, the electric-field peak is displaced into the bulk of the switch, thereby allowing higher electron velocities in the vicinity of the anode. The electric field, as in the abrupt contact case, collapses to the cathode and shifts to the anode during the switching cycle. However, field enhancement at the contacts and under the anode is lower throughout the switching cycle as compared to the abrupt case.

voltage of ≈ 150 V compared to the abrupt contact case (≈ 250 V), as shown in Fig. 2, while using the same amount of optical energy in the switching laser. Since the number of carriers produced is the same in each case, the higher conductivity of the graded contact case results from a higher drift velocity. The higher drift velocity is a consequence of the lower average electric field under the anode compared to the abrupt contact case, as shown in Figs. 4 and 3, respectively ($t=6$ ns). Due to velocity overshoot, the mobility of electrons (and hence the collected current) is larger with the lower field provided the fields exceed the velocity maximum at approximately 3 kV cm^{-1} .

IV. CONCLUDING REMARKS

A model has been developed to investigate the effects of nonuniformities in a GaAs(Si:Cu) photoconductive switch. Results from the model have shown that for a grounded base, electric-field enhancement occurs at the anode during com-

mutation near the peak of the on laser pulse. The electric-field enhancement shifts to the cathode during the closed phase, and then begins to migrate back towards the anode while opening. The high electric field in the opening phase bounds regions of high and low conductivity as electrons are swept into the anode. For the ungrounded abrupt contact, field enhancement occurs near the cathode as well as the anode during the peak of the on laser pulse. These patterns of electric-field enhancement qualitatively agree with experimental observations.⁷ This electric-field enhancement allows gain mechanisms with field thresholds higher than the average field across the switch to become important. Grading near the contacts causes the peak in the electric field to occur in the bulk of the switch rather than at the contacts, resulting in more uniform injection of carriers at the contacts. The reduction in electric field near the contacts allows more current to be collected, as a consequence of velocity overshoot at high electric fields.

ACKNOWLEDGMENTS

The authors would like to thank Professor K. Schoenbach for his helpful advice. This work was supported by BMDO/IST, managed by Office of Naval Research (Contract No. N00014-90-J-1967).

¹ *Gas Discharge Closing Switches*, edited by G. Schaefer, M. Kristiansen, and A. Guenther (Plenum, New York, 1990).

² D. H. Auston, *Semicond. Semimet.* **28**, 85 (1990).

³ *Picosecond Optoelectronic Devices*, edited by C. H. Lee (Academic, New York, 1984).

⁴ R. L. Druce, M. D. Pocha, K. L. Griffin, J. M. Stein, and B. J. O'Bannon, in *8th IEEE International Pulsed Power Conference*, edited by R. White and K. Prestwich (IEEE, New York, 1991), p. 114.

⁵ W. R. Donaldson, L. E. Kingsly, M. Weiner, A. Kim, and R. Zeto, *J. Appl. Phys.* **68**, 6453 (1990).

⁶ K. H. Schoenbach, J. S. Kenney, F. E. Peterkin, and R. J. Allen, *Appl. Phys. Lett.* **63**, 2100 (1993).

⁷ K. H. Schoenbach, J. S. Kenney, and R. J. Allen, *Proc. SPIE* **1632**, 54 (1992).

⁸ F. J. Zutavern, G. M. Loubriel, M. W. O'Malley, W. D. Helgeson, and D. L. McLaughlin, in *8th IEEE International Pulsed Power Conference*, edited by R. White and K. Prestwich (IEEE, New York, 1991), p. 23.

⁹ J. C. Adams, R. Aaron Falk, C. D. Capps, and S. Ferrier, *Proc. SPIE* **1632**, 110 (1992).

¹⁰ E. J. Zutavern, G. M. Loubriel, W. M. O'Malley, L. P. Schanwald, and D. L. McLaughlin, *IEEE Trans. Electron. Devices* **38**, 696 (1991).

¹¹ G. M. Loubriel, M. T. Buttram, W. D. Helgeson, D. L. McLaughlin, M. W. O'Malley, F. J. Zutavern, A. Rosen, and P. J. Stabile, *Proc. SPIE* **1378**, 179 (1992).

¹² G. M. Loubriel, M. W. O'Malley, and F. J. Zutavern, in *6th IEEE Pulsed Power Conference*, edited by P. J. Turchi and B. H. Bernstein (IEEE, New York, 1987), p. 145.

¹³ R. P. Brinkman, K. H. Schoenbach, D. C. Stoudt, V. K. Lakdawala, G. A. Gerdin, and M. K. Kennedy, *IEEE Trans. Electron. Devices* **38**, 701 (1991).

¹⁴ K. H. Schoenbach, V. K. Lakdawala, R. Germer, and S. T. Ko, *J. Appl. Phys.* **63**, 2460 (1988).

¹⁵ P. L. G. Ventzek, R. J. Hoekstra, and M. J. Kushner, *J. Vac. Sci. Technol. B* **12**, 461 (1994).

¹⁶ S. T. Ko, V. K. Lakdawala, K. H. Schoenbach, and M. S. Mazola, in *7th IEEE Pulsed Power Conference*, edited by R. White and B. H. Bernstein (IEEE, New York, 1989), p. 861.

¹⁷ D. C. Stoudt, R. P. Brinkmann, R. A. Roush, M. S. Mazzola, F. J. Zutavern, and G. M. Loubriel, *IEEE Trans. Electron. Devices* **41**, 913 (1994).

¹⁸ S. M. Sze, *Physics of Semiconductor Devices*, 2nd ed. (Wiley, New York, 1981), Chap. 1.